

Neutron Star Phenomenology. Finite Range Simple Effective Interaction Predictions.

X. Viñas,^{a,b,*} P. Bano,^c Z. Naik^c and T.R. Routray^c

^a*Universitat de Barcelona
Barcelona, Spain*

^b*Institut Menorquí d'Estudis
Maó, Spain*

^c*School of Physics, Sambalpur University
Jyotivihar 768011, India*

E-mail: xavier@fqa.ub.edu

We have used the Simple Effective Interaction with a Yukawa form factor to study the neutron star phenomenology. In earlier publications we have reported standard neutron stars properties such as the mass-radius relationship, crust-core transition, global properties of the crust and tidal deformability. In this contribution we want to study the ability of the equations of state built up with this interaction to describe less known properties of the neutron stars such as the threshold mass for prompt collapse in binary neutron star merger, the sound velocity in neutron matter and the gravitational redshift, which are examined in terms of the compactness of the neutron star, the incompressibility and the slope of the symmetry energy. Some of the correlations existing between neutron star properties and the nuclear matter saturation properties have been analyzed and compared with the predictions of other model calculations.

*10th International Conference on Quarks and Nuclear Physics (QNP2024)
8-12 July, 2024
Barcelona, Spain*

*Speaker

1. Introduction

The finite range Simple Effective Interaction (SEI) was proposed by B. Behera and collaborators twenty-five years ago [1] aimed to describe symmetric and asymmetric nuclear matter with emphasis, in particular, on the momentum dependence of the mean field [2]. This effective interaction consist of a finite-range term, in this work of Yukawa type, supplemented by two zero-range terms, one of them density dependent that simulates three-body contributions, plus a zero-range spin-orbit contribution to deal with finite nuclei:

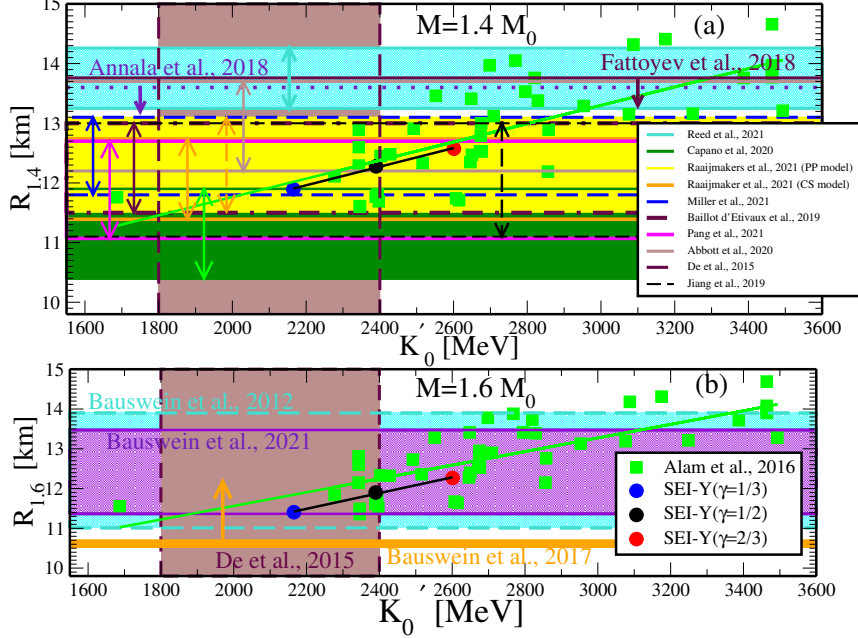
$$\begin{aligned}
 V_{eff} = & t_0(1 + x_0 P_\sigma)\delta(\vec{r}) + \frac{t_3}{6}(1 + x_3 P_\sigma) \left(\frac{\rho(\vec{R})}{1 + b\rho(\vec{R})} \right)^\gamma \delta(\vec{r}) \\
 & + (W + BP_\sigma - HP_\tau - MP_\sigma P_\tau) \frac{e^{-r/\alpha}}{r/\alpha} + \text{Spin-orbit part} \quad (1)
 \end{aligned}$$

The SEI in Eq.(1) has 12 parameters in total, namely, $\alpha, \gamma, b, x_0, x_3, t_0, t_3, W, B, H$, and M plus the spin-orbit strength parameter W_0 , which enters in the description of finite nuclei. Nine combinations of these parameters, $\alpha, \gamma, b, \varepsilon_0^l$ and $\varepsilon_0^{ul}, \varepsilon_\gamma^l$ and $\varepsilon_\gamma^{ul}, \varepsilon_{ex}^l$ and ε_{ex}^{ul} (see Appendix A of Ref.[3]) are needed for a complete description of nuclear matter (NM) as well as the $npe\mu$ neutron star matter (NSM). These nine parameters are determined in NM using experimental and empirical constraints of very generic nature. In particular, we have used the experimental constraint of vanishing mean field for kinetic energy of the nucleon of 300 MeV [4, 5], which allow to determines the range, α and the exchange strength parameters ε_{ex}^l and ε_{ex}^{ul} . The protocol adopted for the parameter fixation lies has two main advantages. On the one hand, the NM incompressibility at saturation, K_0 , governed by the parameter γ , can be varied without affecting the momentum dependence of the mean field in SNM. On the other hand, the slope of the symmetry energy L can be varied without changing the isoscalar properties and the $n-p$ effective mass splitting. The parameters of SEI, thus determined can give the trend of the predictions of the microscopic Dirac-Brueckner-Hatree-Fock and variational calculations using realistic interactions.

SEI has been applied in the former studies of symmetric and asymmetric nuclear matter (SNM and ANM, respectively) at zero and finite temperature as well as to describe finite nuclei (see [3] and references therein). In the astrophysical domain we have studied the thermal evolution of nuclear symmetry energy [6] and the equation of state of charge neutral hot isentropic $npe\mu$ NSM in β -equilibrium [12]. Using SEI standard neutron star (NS) properties such as the mass-radius relationship [10], obtained by solving the Tolman-Oppenheimer-Volkov (TOV) equation, the the crust-core transition and crustal properties [7, 8], the tidal deformability [11] and the r -mode instability [9, 10] have been analyzed.

In this contribution we briefly summarize the main findings discussed in detail in Ref.[3] about some constraints in neutron stars resulting from recent studies, such as the threshold mass for prompt collapse in binary neutron star merger, the sound speed in NSM and the gravitational redshift. We will also analyze some correlations existing between NSM properties and the NM saturation properties.

Figure 1: $R_{1.4}$ of $1.4 M_{\odot}$ neutron stars and (b) Radii $R_{1.6}$ of $1.6 M_{\odot}$ neutron stars versus the slope of the incompressibility K'_0 obtained using different EoS of SEI having $\gamma=1/3, 1/2,$ and $2/3$.



2. Slope of the incompressibility and Radius of Neutron star

In Ref.[13] it is claimed that the NS radius is very well correlated with a linear combination of the slope with respect to the density of the incompressibility, K'_0 , and the symmetry energy, L , computed both at normal saturation density in SNM ρ_0 , which is almost independent of the mass of the NS in the range $0.6-1.8 M_{\odot}$. However, in Figure 1 we display the radius of the NS, computed by solving the TOV equation for the NS of masses 1.4 and $1.6 M_{\odot}$ using SEI EOS with $\gamma=1/3, 1/2,$ and $2/3$, as a function of the slope of the incompressibility in SNM, K'_0 . In the same Figure the values predicted by a large set of 44 EOS provided by relativistic and non-relativistic models reported in [13] are also plotted. The color bands correspond to different estimates available in the literature. We refer the reader to [3] for further details. From this Figure we see that the models of [13] show a moderate linear correlation whereas the three SEI models show a strong correlation for both NS masses. This is probably due to the fact that the models used in [13] are of very different nature, which is not the case of SEI. We also have checked that the NS radius provided by SEI are also correlated with the combination of K'_0 and L mentioned before.

3. Neutron star merger and incompressibility of ANM

As has been pointed out in earlier literature (see [3] for details), the threshold mass, M_{th} , of a NS for prompt collapse (PC) to form a black hole (BH) in the binary neutron

Table 1: Threshold mass M_{th} for the three EoSs of SEI($\gamma=1/3$, $1/2$, and $2/3$) using the values of constants a and b from literature, given in Table II of Ref. [14].

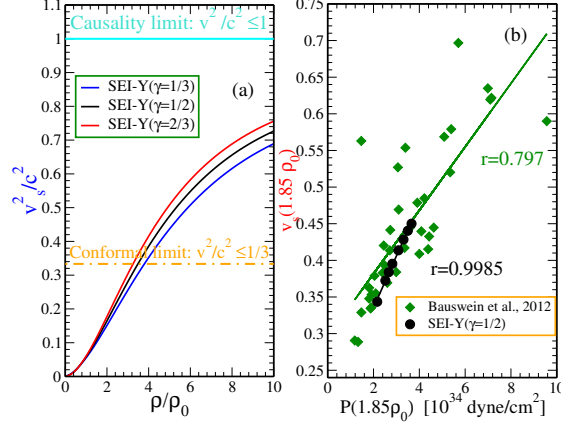
SEI-Y($\gamma = 2/3$)					
a	b	R_{max}^{TOV}	C_{max}^{TOV}	κ	M_{th}
-3.342	2.42	10.523	0.275	1.499	2.937
-3.38	2.43	10.523	0.275	1.498	2.936
$-3.36^{+0.20}_{-0.20}$	$2.35^{+0.06}_{-0.06}$	10.523	0.275	$1.424^{+0.115}_{-0.115}$	$2.790^{+0.225}_{-0.225}$
SEI-Y($\gamma = 1/2$)					
a	b	R_{max}^{TOV}	C_{max}^{TOV}	κ	M_{th}
-3.342	2.42	10.243	0.272	1.5095	2.846
-3.38	2.43	10.243	0.272	1.5091	2.845
$-3.36^{+0.20}_{-0.20}$	$2.35^{+0.06}_{-0.06}$	10.243	0.272	$1.434^{+0.114}_{-0.114}$	$2.705^{+0.215}_{-0.215}$
SEI-Y($\gamma = 1/3$)					
a	b	R_{max}^{TOV}	C_{max}^{TOV}	κ	M_{th}
-3.342	2.42	9.943	0.267	1.5252	2.7437
-3.38	2.43	9.943	0.267	1.5250	2.7434
$-3.36^{+0.20}_{-0.20}$	$2.35^{+0.06}_{-0.06}$	9.943	0.267	$1.45^{+0.113}_{-0.113}$	$2.609^{+0.204}_{-0.204}$

star merger (BNSM) scales with the maximum mass, M_{max} , of the non-rotating NS as $M_{th} = \kappa M_{max}$, where the scaling factor κ is strongly correlated with the compactness C_{max} as $\kappa = aC_{max} + b$. The compactness, defined as $C_{max} = GM_{max}/c^2 R_{max}$, is computed with the M_{max} and R_{max} solution of the TOV equation for the considered NS. Using the parameters a and b given in the first column of Table 2 (taken from Table II of Ref.[14]), we display in Table 2 the M_{th} for PC in BNSM computed with the SEI EOS with $\gamma=1/3$, $1/2$, and $2/3$. In the case of a delayed/no collapse, the estimated total binary mass of GW170817 ($M_{tot}^{GW170817} = 2.74^{+0.04}_{-0.01}$) provides a lower bound on the M_{th} for direct BH formation. The M_{th} values predicted by SEI EOSs for the three sets of a and b parameters conform to this limiting value.

4. Sound speed in neutron star matter

The adiabatic speed of the sound in ANM evaluated at constant entropy is given by $\frac{v_s^2}{c^2} = \frac{K(\rho, \delta)}{9(mc^2 + e(\rho, \delta) + P(\rho, \delta)/\rho)}$ (see [3] and references therein), where $K(\rho, \delta)$, $e(\rho, \delta)$ and $P(\rho, \delta)$ are the incompressibility, energy per nucleon and pressure, respectively, in ANM with isospin asymmetry δ , which for each density ρ is obtained from the β -stability condition. The square of the sound velocity computed with three different SEI EOS ($\gamma=1/3$, $1/2$, and $2/3$) is displayed as a function of the density in the left panel of Figure 2. The square of the speed is larger for larger values of the γ parameter, i.e. for larger values of K_0 , of the SEI EOS, as expected. We also see that in the three considered cases, $K(\rho, \delta)$ increases with growing density without exceeding the causality limit. In the right panel of Figure 2 we display the speed of the sound in NSM as a function of the nucleonic pressure computed at a density $1.85\rho_0$ with the SEI EOS having $\gamma=1/2$ and different values of the slope of the symmetry energy L in the range 60-110 MeV together with the predictions of the set

Figure 2: Left: Speed of sound in NSM as a function density for SEI EOS with $\gamma = 1/3, 1/2, 2/3$. Right: At central density $1.85\rho_0$ as a function of pressure. The dots correspond to different SEI EoS with $\gamma=1/2$ and slope parameter L in the range 60-110 MeV.



of EOS used in [15]. The SEI predictions show a nice linear correlation between the square of the velocity of the sound and the pressure, which is deteriorated in the case of the EOS used in [15] probably due to the different nature of the EOS considered in this latter case.

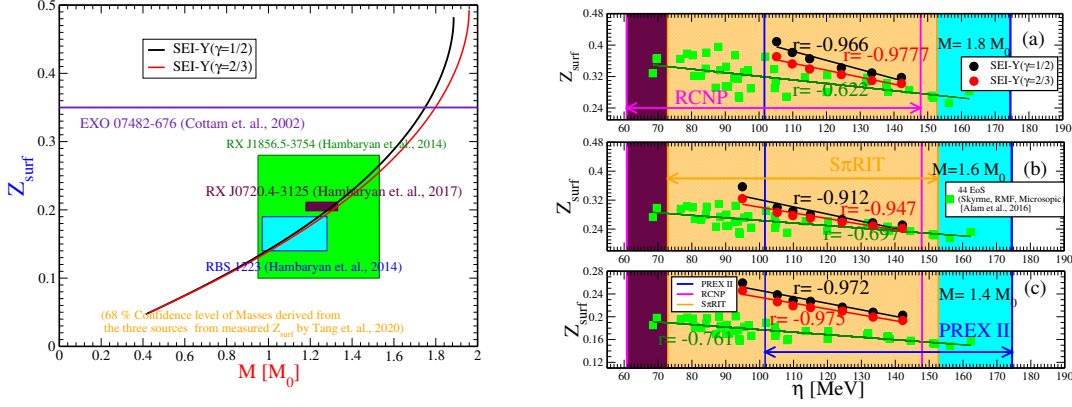
5. Gravitational Red shift

The gravitational redshift of a signal from the star surface is defined as $Z_{surf} = \left(1 - \frac{2GM}{c^2 R}\right)^{-1/2} - 1$. The measure of this quantity can provide direct insight into the compactness of the NS and therefore can constrain the EOS for dense matter. The left panel of Figure 3 displays Z_{surf} as a function of the NS mass. The shaded area in the figure collects the observational information provided by the RBS 1223, RX J0720.4-3125 and RX J1856.5-3754 NS (see [3] for additional information). The predictions of the SEI model with $\gamma = 1/2$ and $\gamma = 2/3$ displayed in this panel show that Z_{surf} grows with increasing mass of the NS. For low masses both SEI predictions coincide, but they differ for high mass, which shows the dependence of Z_{surf} on incompressibility in SNM, 237.74 ($\gamma = 1/2$) and 263.14 ($\gamma = 2/3$). However, both the EoSs conform in the constraints provided by the three NSs. The right panel of Figure 3 Z_{surf} is plotted as a function of the parameter $\eta = (K_0 L^2)^{1/3}$ for NS of 1.8, 1.6 and 1.4 M_\odot . The SEI values for $\gamma = 1/2$ and $\gamma = 2/3$ show a rather strong anticorrelation between Z_{surf} and η , while for the set of models of [13] the anticorrelation is much weaker, probably due to the different nature of the models considered.

6. Summary

In this study we have discussed some recent phenomenology of neutron stars related to the binary neutron star merger and the gravitational redshift using using the effective

Figure 3: Z_{surf} predicted by the SEI-Y ($\gamma = 1/2$) and SEI-Y ($\gamma = 2/3$) EoSs. Left: As a function of the NS mass. Right: As a function of the parameter η . Shaded regions correspond to observational data (see [3] for details). The green diamonds are the data for the 44-EoSs reported in [13].



SEI-Y interaction. Specifically, this model predicts a linear correlation between the radii of neutron stars with 1.4 and 1.6 M_{\odot} and the slope (derivative respect to the density) of the incompressibility modulus. Also predicts the threshold mass for prompt collapse of neutron stars in agreement with data extracted from the GW170817 event. Using the SEI-Y model, the speed of the sound, computed at given values of the density and incompressibility modulus for different values of the slope of the symmetry energy, shows a linear correlation with the pressure. The gravitational redshift of a signal emitted from the star surface calculated with the SEI-Y model is found to be in agreement with the observational information provided by several pulsars, on the one hand, and show an anticorrelation with the parameter η defined in the main text, on the other hand. Since the SEI-Y model is able to predict recent neutron star phenomenology in good agreement with the observational data, it could be considered as a possible candidate for simulation studies in the binary neutron star merger as well as in supernovae leading to the formation of proto-neutron stars.

References

- [1] B. Behera, T.R. Routray and R.K. Satpathy, *J. Phys. G: Nucl. Part. Phys* **24**, 2073 (1998).
- [2] B. Behera, T.R. Routray, et al., *Nucl. Phys A* **753**, 367 (2005).
- [3] X. Viñas, P. Bano, Z. Naik and T.R. Routray, *Symmetry* **16**, 215 (2024).
- [4] G.M. Welke, M. Prakash, T.T.S. Kuo, S. Das Guptan and C. Gale, *Phys. Rev. C* **38**, 2101 (1988).
- [5] L.P. Csernai, G. Fai, C. Gale and E. Oesnes, *Phys. Rev. C* **46**, 736 (1992).

- [6] B. Behera, T.R. Routray and S.K. Tripathy, *J. Phys. G: Nucl. Part. Phys.* **36**, 125105 (2009).
- [7] T.R. Routray, X. Viñas, et al., *J. Phys. G: Nucl. Part. Phys.* **43**, 105101 (2016).
- [8] C. Gonzalez-Boquera, M. Centelles, X. Viñas, and T.R. Routray, *Phys. Rev. C* **100**, 015806 (2019).
- [9] S.P. Pattnaik, T.R. Routray, et al., *J. Phys. G: Nucl. Part. Phys.* **45**, 055202 (2018).
- [10] T.R. Routray, S.P. Pattnaik, et al., *Phys. Scr.* **96**, 045301 (2021)
- [11] P. Bano, S.P. Pattnaik, M. Centelles, X. Viñas and T. R. Routray, *Phys. Rev. C* **108** (2023) 015802.
- [12] T.R. Routray, S. Sahoo, X. Viñas, D.N. Basu and M. Centelles, *J. Phys. G: Nucl. Part. Phys.* **51**, 085203 (2024).
- [13] N. Alam, B.K. Agrawal et al., *Phys. Rev. C* **90**, 054317 (2016).
- [14] R. Kashyap, A. Das, et al., *Phys. Rev. D* **105**, 103022 (2022).
- [15] A. Bauswein, H.-T. Janka, K. Hebeler and A. Schwenk, *Phys. Rev. D* **86**, 063001 (2012).